

ALLWAS: Active Learning on Language models in WASSerstein space

Anonymous ACL submission

Abstract

Active learning has emerged as a standard paradigm in areas with scarcity of labeled training data, such as in the medical domain. Language models have emerged as the prevalent choice of several natural language tasks due to the performance boost offered by these models. However, in several domains, such as medicine, the scarcity of labeled training data is a common issue. Also, these models may not work well in cases where class imbalance is prevalent. Active learning may prove helpful in these cases to boost the performance with a limited label budget. To this end, we propose a novel method using sampling techniques based on submodular optimization and optimal transport for active Learning in language models, dubbed ALLWAS. We construct a sampling strategy based on submodular optimization of the designed objective in the gradient domain. Furthermore, to enable learning from few samples, we propose a novel strategy for sampling from the Wasserstein barycenters. Our empirical evaluations on standard benchmark datasets for text classification show that our methods perform significantly better ($> 20\%$ relative increase in some cases) than existing approaches for active learning on language models.

1 Introduction

Active learning is a technique for improving model performance over a fixed annotation budget (Cohn et al., 1996). Generally, the data is obtained for labeling iteratively after alternating training phases until the desired performance is achieved. This contrasts with passive learning, where one assumes access to labels for the entire pool of data. There are three scenarios for active learning (Settles, 2009): (1) *pool-based*, where a set of unlabeled data points are available (2) *stream-based*, in which the data points are received in an online fashion, and (3) *membership query synthesis*, where the data points are generated for labeling.

In this work, our focus will be on the pool-based setting for active learning.

Active learning has benefited a wide gamut of applications such as text classification (Tong and Koller, 2002; Hoi et al., 2006), named entity recognition (Tomanek and Hahn, 2009; Shen et al., 2004), and machine translation (Haffari and Sarkar, 2009), to name a few. Transformer-based language models (Devlin et al., 2019) have shown improved performance on NLP tasks. These models with a large number of parameters require comparable amounts of data to produce good results (Margatina et al., 2021) and thus pose a challenge in the active learning setting. There has been a recent surge in the study of language models in the active learning setup (Ein-Dor et al., 2020; Margatina et al., 2021). However, many of these approaches are based on uncertainty sampling, which may not work well for uncalibrated deep models (Guo et al., 2017). Other approaches look at the embedding space (Sener and Savarese, 2018) or the gradient space (Huang et al., 2016). However, these methods generally assume a Euclidean metric between the data points in the respective spaces, which fails to judiciously capture the complex interactions. In this paper, we hypothesize that finding a core set of points using the Wasserstein metric would result in better performance than simply selecting a set of points that minimizes or maximizes a measure.

Such large language models require considerable amounts of representative data, which makes it infeasible for fine-tuning in the active learning scenario that work with a limited annotation budget. This drawback is effectively alleviated by *data augmentation* in the image domain (Ratner et al., 2017). However, data augmentation is not a straightforward exercise for textual data. There have been numerous attempts to augment data by generating samples to label in the *token space* (Liu et al., 2020; Quteineh et al., 2020) and the *feature*

space (Kumar et al., 2019b; Feng et al., 2021). Generating tokens could render the labels erroneous because of the nature of the hard assignment. To this end, we propose an over-sampling strategy based on *Wasserstein barycenters* (Curti and Doucet, 2014) in the embedding space. Our rationale here is that augmenting data by such a sampling technique benefits active learning because it operates well in both the *low data regime* as well as the *class imbalance* scenarios.

To the best of our knowledge we are the first to propose such an augmentation method for active learning with language models. Our key contributions are:

1. We propose a novel sampling strategy based on the Wasserstein distance in the gradient space. We prove its submodularity and propose a $1 - \frac{1}{e}$ optimal greedy algorithm.
2. We design an over-sampling technique based on the Wasserstein barycenter of the embeddings of the data points for better performance in the cases with few labeled samples.
3. We demonstrate the effectiveness of our method by running extensive experiments on real world scenarios of few labeled samples and class imbalance. We also conduct experiments on the multi-class settings which have not been considered in previous works.

2 Related Work

Prior works on active learning have focused on uncertainty based sampling such as entropy (Lewis and Gale, 1994), least model confidence (Settles et al., 2008) and diversity based methods (Settles et al., 2008; Xu et al., 2007; Wei et al., 2015). (Settles et al., 2008; Hsu and Lin, 2015) have tried to use a combination of the diversity and uncertainty based approaches. Active learning has been effectively used in previous works for CNN based models (Sener and Savarese, 2018; Gal and Ghahramani, 2016; Gissin and Shalev-Shwartz, 2019). *Coresets* have been used for importance sampling (Cohen et al., 2017), *k*-means and medians clustering (Har-Peled and Mazumdar, 2004) and for Gaussian mixture models (GMMs) (Lucic et al., 2018). Work in (Mirzasoleiman et al., 2020) used coresets in the gradient domain for subsampling data points for accelerated training. (Wei et al., 2015) combines the uncertainty sampling methods with a submodular optimization method for subset selection. (Ramalingam et al., 2021) uses a combi-

nation of submodular functions for balancing constraints of class labels and decision boundaries using matroids. A study of the theoretical performance of batch mode active learning with submodularity is given in (Chen and Krause, 2013). Submodular functions have also been used in NLP for text summarization (Lin and Bilmes, 2011), machine translation (Kirchhoff and Bilmes) and goal oriented chatbots (Dimovski et al., 2018). In contrast to previous works we propose a novel submodular function for query sampling that operates in the gradient space. We argue that this would help select samples that are most representative of the gradients.

Data Augmentation techniques using Wasserstein barycenters and optimal transport have been adopted in the literature (Zhu et al., 2020; Bessalov et al., 2021; Nadeem et al., 2020; Yan et al., 2019) for the image domain. In contrast, NLP researchers have primarily focused on generating data in the token space (Liu et al., 2020; Quteineh et al., 2020) for data augmentation (Wang and Yang, 2015; Kobayashi, 2018), paraphrase generation (Kumar et al., 2019a) etc. There exist methods that use *mixups* in the feature space (Kumar et al., 2019b; Feng et al., 2021) for data augmentation. However, to the best of our knowledge this is the first work to explore data augmentation using Wasserstein barycenters for active learning using language models. We argue that our method is advantageous in the low sample and imbalanced class settings.

3 Problem Statement and Approach

3.1 Problem Formulation

Typical pool based active learning methods have the following components: a pool of unlabelled data U_{pool} , a model M on which to train the data for the downstream task, and an annotation budget b , which is a limit on the amount of labeled data that can be obtained. The last component is an acquisition or query function $q(\cdot)$ that would be used for querying over U_{pool} to obtain the data to be labeled. This is an iterative process in which, at every iteration, the query function $q(\cdot)$ acquires a query set of size $k (< b)$. Finally, the model M is trained over the samples provided by the query function and is evaluated on a validation set D_{val} . The aim is to maximize the performance on D_{val} with a minimum labeled sample set (Siddhant and Lipton, 2018). The process is repeated until the

annotation budget b is exceeded or the desired performance on the validation set is achieved.

3.2 Approach

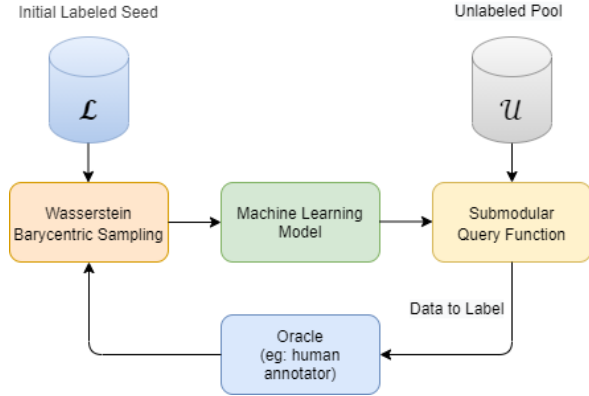


Figure 1: ALLWAS Process Flow. It uses Wasserstein Barycenters for data augmentation. The submodular query function is used for unlabeled data acquisition. These two steps aims to enhance performance of underlying ML model (BERT in our case).

Figure 1 outlines the flow of our proposed approach. First, the initial labeled seed of data is given to the barycentric sampling module for up-sampling. Next, a model, in this case, a language model, is trained on this initial seed. The query function then uses the model to sample data points labeled by an oracle and a human annotator. The newly labeled data points are fed to the upsampling module, and the process repeats until the labeling budget is reached or the desired performance is achieved. The details of the individual components, along with some preliminaries, are explained in the following sections.

3.2.1 Optimal Transport and Wasserstein Barycenters

Let Ω be any space, D be a distance metric in Ω , and $P(\Omega)$ be the set of probability measures in that space. Let $x, y \in \Omega$ be the dirac masses with probability measures μ and ν respectively. The Optimal transport (Monge, 1781) problem is to minimize the cost in transporting x to y . The Wasserstein distance defines the optimal transport plan to move an amount of matter from one location to another.

Definition 3.1. Let $p \in [1, \infty)$ and $D: \Omega \times \Omega \rightarrow [0, \infty)$ be the cost of transporting the measure μ to ν , then the p^{th} Wasserstein distance (Villani)

between the measures is given by

$$W_p(\mu, \nu) = \inf_{\gamma \in \Pi(\mu, \nu)} \left(\int_{\Omega \times \Omega} D(x, y)^p d\gamma \right)^{\frac{1}{p}} \quad (1)$$

where Π is the set of all the possible transport plans with the marginals μ and ν .

Definition 3.2 (Wasserstein Barycenter, (Agueh and Carlier, 2011)). A Wasserstein barycenter of n measures $\{v_1, v_2, \dots, v_n\}$ in $\mathbb{P} \subset P(\Omega)$ is a measure that minimizes the weighted sum of the p^{th} Wasserstein distance over \mathbb{P} i.e. it is a minimiser of f defined as below

$$f(\mu) = \sum_{i=1}^N \lambda_i W_p^p(\mu, \nu_i) \quad (2)$$

Here we consider a convex combination of W_p^p i.e. $\lambda_i \leq 1$ and $\sum_i \lambda_i = 1$. If D is the L_2 distance and $p = 2$ that is when $P(\Omega, D)$ is the euclidean distance metric, minimizing f results in the k means solution (Kaufman and Rousseeuw, 1987).

Sampling using Wasserstein Barycenters: The definition of the Wasserstein barycenter in 3.2 allows us to sample from a set of data points as illustrated in this section. The intuition for us-

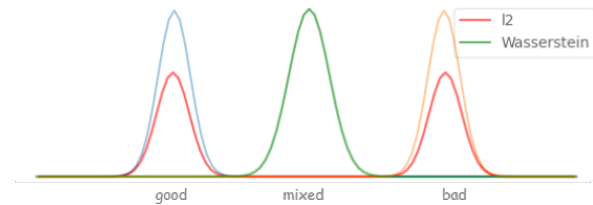


Figure 2: Example of a 1D Distribution (in orange and blue) showing the Wasserstein and ℓ_2 barycenters

ing Wasserstein barycenters instead of euclidean barycenters is outlined in Figure 2. The figure shows a distribution of 1-dimensional word vectors, with the words "good" and "bad" at the extremes and the word "mixed" in between them. We see from the distribution that the data contains the words "good" and "bad". Sampling using the Wasserstein barycenter with equal weights gives us the word "mixed." In contrast, the ℓ_2 barycenter would sample either of the words "good" or "bad" with equal probability. This implies that in a sentiment classification task, a pair of sentences "The movie was good" and "The movie was bad" would enable us to sample a neutral sentence "The movie was mixed" using the Wasserstein barycenter. We argue that in contrast to sampling from the ℓ_2 barycenter (see subsection 5.4) or no over-

sampling (augmentation), sampling technique incorporating Wasserstein barycenters would result in superior performance for the few sample and imbalanced case.

Consider an machine learning (language) model such as Bert (Devlin et al., 2019) with the output d dimensional contextual embeddings as e_1, e_2, \dots, e_n from a layer l for the input tokens w_1, w_2, \dots, w_n respectively. Now let us consider s sentences each with number of tokens given by n_1, n_2, \dots, n_s respectively. The contextual embeddings of a sentence s_i would be represented as $E_i = [e_1, e_2, \dots, e_{n_i}]$, where $E_i \in R^{d \times n_i}$. The Wasserstein barycenter of these samples would then be given by,

$$E_c = \underset{E_c \in R^{d \times n_i}}{\operatorname{argmin}} \sum_{i=1}^N \lambda_i W_p^p(E_c, E_i) \quad (3)$$

Thus, we obtain the barycenter in the embedding space. We also modify the labels by taking a weighted average as follows:

$$L_c = \sum_{i=1}^N \lambda_i L_i \quad (4)$$

Where L_i is the true class probabilities of the sentence s_i . Varying the values of the λ s could enable picking multiple data points, enabling over-sampling from the pool of labeled data.

3.2.2 Submodular Acquisition function

Let V be the set of all points in the space Ω under consideration. Let A, B be two subsets of V such that $A \subseteq B$. Let F be a set function (acting on a set S) $\Omega^{|S|} \rightarrow R$, then F is said to be submodular if, on adding an element $e \in V \setminus B$ to A and B , it satisfies the below condition

$$F\{A \cup e\} - F\{A\} \geq F\{B \cup e\} - F\{B\}$$

Previous works have used gradient spaces for subset selection in active learning (Huang et al., 2016) and to speed up training (Mirzasoleiman et al., 2020). Selecting a subset of points with gradients that are representative of the gradients of the entire set of points would intuitively result in steering the model parameters in the right direction of the optimum value. This motivates our approach of using the gradient space to perform the acquisition of the data points. One issue that remains is that unlike in (Mirzasoleiman et al., 2020) we do not have the true labels beforehand. (Huang et al., 2016) proposes to use the expected gradient length with the expectation over the predicted logits. However, the predicted probabilities do not

always correlate with the model confidence (Guo et al., 2017) and calibration of the model may be required. We differ in our approach where we use the Wasserstein distances between the points in the gradient space to find the most representative sample set. Specifically, we select the subset that minimizes the below function.

$$L\{S\} = \sum_{i \in V} \min_{j \in S} (W_p^p(i, j)) \quad (5)$$

where $W_p^p(i, j)$ is the p^{th} Wasserstein distance between the i^{th} and the j^{th} sample in the gradient space. Minimizing L is equivalent to finding the k medoids (Kaufman and Rousseeuw, 1987) and in general, finding an exact solution is an NP-Hard problem. However, optimizing a submodular function enables us to obtain a $1 - \frac{1}{e}$ optimal (Nemhauser et al.) solution in a greedy manner. We define a submodular function using L as below:

$$F\{S\} = L\{s_0\} - L\{s_0 \cup S\} \quad (6)$$

Here s_0 is an auxiliary set element and $L\{s_0\}$ can be considered a constant. We prove the submodularity of equation 6 below.

Lemma 3.1. *The function $L\{S\}$ is monotone decreasing.*

Proof. From the definition of L we have,

$$L = \sum_{i \in V} \min_{j \in S} (W_p^p(i, j))$$

where $W_p^p(i, j)$ is the p^{th} Wasserstein distance in the gradient space. On adding an element $e \in V \setminus S$ to S , we get the new set $S' = S \cup e$. The metric for the new set then becomes $L' = \sum_{i \in V} \min_{j \in S'} (W_p^p(i, j))$. Now let's assume

that $L' > L$. This means that for some point $i \in V$, the newly added point e was selected and the distance $W_p^p(i, e)$ is greater than the previous minimum $W_p^p(i, j)$, which is a contradiction. Thus, we have that $L' \leq L$. \square

Corollary 3.1. *The function $F = L\{s_0\} - L\{S \cup s_0\}$ is monotone increasing.*

Proof. If we fix $L\{s_0\}$ to a constant and since $L\{S\}$ is monotone decreasing from lemma 3.1, we have F is monotone increasing. \square

Proposition 3.1. *The rate of increase of F at $A \in V$ is greater than or equal to that at $B(\in V) \supseteq A$.*

To understand proposition 3.1 we note that adding $e \in V \setminus B$ to A causes an increase in F

or maintains the value as it is monotone increasing from corollary 3.1 and since $A \subseteq B$ adding e to B will only cause the same or lesser increase in $F\{B\}$ by definition of F .

Theorem 3.1. F is a submodular function.

Proof. Assume set of points in the gradient space, $B \in V$ and a set $A \subseteq B$. We assume a continuous space of the elements such that adding a fraction of it would cause a fractional change in the output. Note that an interpolation does not change the function definition for the discrete case where the direct mass is concentrated. Consider adding an element(s) $e \in V \setminus B$ to the sets A and B . By the gradient theorem for path integral we get,

$$\begin{aligned} F(A \cup e) - F(A) &= \int_0^1 \frac{\partial F(A + \alpha(A \cup e - A))}{\partial \alpha} d\alpha \\ &= \int_0^1 \frac{\partial F(A + \alpha(A \cup e - A))}{\partial x} \frac{\partial x}{\partial \alpha} d\alpha \\ &\quad \text{(using chain rule)} \\ &= (A \cup e - A) \int_0^1 \frac{\partial F(A + \alpha(A \cup e - A))}{\partial x} d\alpha \\ &\quad \text{(as } \frac{\partial x}{\partial \alpha} = A \cup e - A = \text{constant } K) \\ &= K \int_0^1 \frac{\partial F(A + \alpha(A \cup e - A))}{\partial x} d\alpha \end{aligned}$$

Similarly,

$$F(B \cup e) - F(B) = K \int_0^1 \frac{\partial F(B + \alpha(B \cup e - B))}{\partial x} d\alpha$$

From proposition 3.1 we have $\frac{\partial F(A)}{\partial x}|_{x=A} \geq \frac{\partial F(B)}{\partial x}|_{x=B}$ for addition of the same element e and this will be true in the entire interval $\alpha \in [0, 1]$. Thus we get,

$$F(A \cup e) - F(A) \geq F(B \cup e) - F(B)$$

Thus we can conclude that F is submodular. \square

Since we have a submodular function in F , we could use a greedy algorithm to find a set that is $(1 - \frac{1}{e})$ of the optimal set S that maximizes F (minimizes L). It further runs in polynomial time. The greedy algorithm begins with an empty set $S = \phi$ and at each iteration keeps adding an element $e \in V \setminus S$ that maximizes $F(e|S_{i-1}) = F(e \cup S_{i-1}) - F(S_{i-1})$ i.e. $S_i = S_{i-1} \cup \underset{e \in V}{\operatorname{argmax}} F(e|S_{i-1})$. The iterations continue till a specified labeling budget is attained. In practice, computing the gradients with respect to the entire set of weights could be computationally

expensive in language models that could have millions of parameters. Fortunately for deep networks most of the variation in gradients with respect to the loss is captured by the last layer (Katharopoulos and Fleuret, 2019). Also, Mirzasoleiman et al. (2020) efficiently upper bounds the norm of the difference between the gradients by the norm of the gradients of the loss with respect to the inputs to the last layer. Thus for computational efficiency we restrict to finding the gradients with respect to the weights of the last layer. The outline is sketched in Algorithm 1.

Algorithm 1: Greedy Algorithm to sample from the pool of unlabeled data points for Active learning

Input: Unlabeled pool \mathcal{U} , Total Budget B , Samples to label per iteration k , Model M , Initial labeled set \mathcal{L} ;

while $|\mathcal{L}| \leq |B|$ **do**

- Train model M on \mathcal{L}
- $V \leftarrow \phi$
- for** $x \in \mathcal{U}$ **do**
- $e \leftarrow \frac{\partial \mathcal{M}(x)}{\partial x}$
- $V = V \cup e$
- end**
- $S_0 \leftarrow \mathcal{L}$
- **for** $i = 1, 2, \dots, k$ **do**
- $e = \underset{e \in V}{\operatorname{argmax}} F(e|S_{i-1})$
- $S_i = S_{i-1} \cup e$
- end**
- $L \leftarrow S$

end

4 Experimental Setup

4.1 Datasets

We use 7 standard text classification datasets and their 10 variants as used by (Ein-Dor et al., 2020). Specifically, the datasets used are Wiki Attack (Wulczyn et al., 2017), ISEAR (Shao et al., 2015), TREC (Li and Roth, 2002), CoLA (Warstadt et al., 2019), AG’s News (Zhang et al., 2015), Subjectivity (Pang and Lee, 2004), and Polarity (Pang and Lee, 2005). The experimental setup considers three settings: (1) **Balanced**, in which the prior probability of a class occurrence is $\geq 15\%$. Here the initial seed for labeling is obtained by random sampling. (2) **Imbalanced** and (3) **Imbalanced practical** in which the prior probability of a class occurrence is $\leq 15\%$. The initial seed for labeling

411 is obtained by assuming a high precision algorithm
412 or a query. For more details on the datasets and ex-
413 perimental setups, we refer the readers to (Ein-Dor
414 et al., 2020) and the Appendix.

415 4.2 Comparative Methods

416 The acquisition methods are used to query and ob-
417 tain samples from the unlabeled pool for labeling.
418 In the implementation 25 samples are queried per
419 iteration. We use the active learning acquisition
420 strategies as in (Ein-Dor et al., 2020) namely **Ran-**
421 **dom, Least Confidence (LC, (Lewis and Gale,**
422 **1994)), Monte Carlo Dropout (Dropout, (Gal**
423 **and Ghahramani, 2016)), Perceptron Ensemble**
424 **(PE, (Ein-Dor et al., 2020)), Expected Gradient**
425 **Length (EGL, (Huang et al., 2016)) , Core-Set**
426 **((Sener and Savarese, 2018)), Discriminative Ac-**
427 **tive Learning (DAL, (Gissin and Shalev-Shwartz,**
428 **2019)).** For details refer to the Appendix.

429 4.3 Implementation Details

430 The BERT_{BASE} model (110 M parameters) is used
431 with a batch size of 50 and a maximum token
432 length of 100 tokens. In each active learning it-
433 eration, the model is trained for five epochs from
434 scratch. A learning rate of 5×10^{-5} has been used.
435 The other parameters are the same as in the Py-
436 Torch implementation of BERT. We run each ac-
437 tive learning method for five runs starting from the
438 same initial seed (of 25 samples) for every model
439 for a given run and average the result as in (Ein-
440 Dor et al., 2020).

441 5 Results and Discussion

442 We aim to answer the below Research Questions:

- 443 1. **RQ1:** Is ALLWAS beneficial in the low re-
444 source and imbalanced setting?
- 445 2. **RQ2:** Does the proposed Wasserstein
446 barycentric over-sampling help in the few
447 sample settings compared to the control of no
448 over-sampling?
- 449 3. **RQ3:** Does the proposed gradient-domain
450 submodular query function perform better
451 than existing approaches in the same space?
- 452 4. **RQ4:** Is barycentric over-sampling in the
453 wasserstein space significantly better than
454 that in the ℓ_2 space?

455 5.1 Active Learning Results on the Binary 456 class settings

457 The results, for the imbalanced practical binary
458 setting, are shown in the graphs in figures 10. The

459 results for the other settings can be found in the
460 Appendix. For brevity we show the results on the
461 same set of the active learning methods as in (Ein-
462 Dor et al., 2020). From the Figures in 10, we ob-
463 serve that in most of the datasets our method out-
464 performs all the other methods in all settings. For
465 the balanced setting, we find that our method per-
466 forms exceptionally well in the start with lesser
467 data. Then as the training data increases with it-
468 erations, the performance of the other methods
469 catches up. Thus we could say that our method
470 converges faster in scenarios where the data is bal-
471 anced. In the two imbalanced settings, we observe
472 an apparent gain in performance. Thus, we con-
473 clude that combining submodular query function
474 and barycentric sampling benefits performance in
475 class imbalance cases of active learning (answer-
476 ing **RQ1**).

477 5.2 Few Sample Results

478 In the few sample settings, we test the barycentric
479 sampling on a few data points sampled incremen-
480 tally. The augmentation factor is kept at 20 as a
481 default. The results are plotted in Figure 4. We ob-
482 serve a stark improvement in the results, in some
483 cases the relative increase being as high as 24%.
484 This shows that in such cases of data scarcity, the
485 task, in this case, classification, could benefit by
486 sampling from the Wasserstein barycenter of the
487 original samples as an augmentation technique in-
488 dependent of the sampling technique used in the
489 query function (answering **RQ2**).

490 5.3 Coreset vs Maximum Gradient

491 In this section, we study the performance of our
492 query function (ALLWAS w/o Augmentation) that
493 selects a coreset of the gradients against the ex-
494 pected gradient length method that picks sam-
495 ples with the largest expected gradient magnitudes
496 (EGL, (Huang et al., 2016)). The plots in figure
497 5 show that our query sampling technique outper-
498 forms the EGL method. Thus we conclude that
499 selecting core-sets is the better approach against
500 picking samples with extreme values in the gradi-
501 ent domain in assertion of **RQ3**.

502 5.4 Sampling from Wasserstein vs ℓ_2 503 barycenter

504 In order to confirm the claim made in subsec-
505 tion 3.2.1, we perform a comparison between
506 ℓ_2 barycentric and Wasserstein barycentric over-
507 sampling on the imbalanced practical setting.

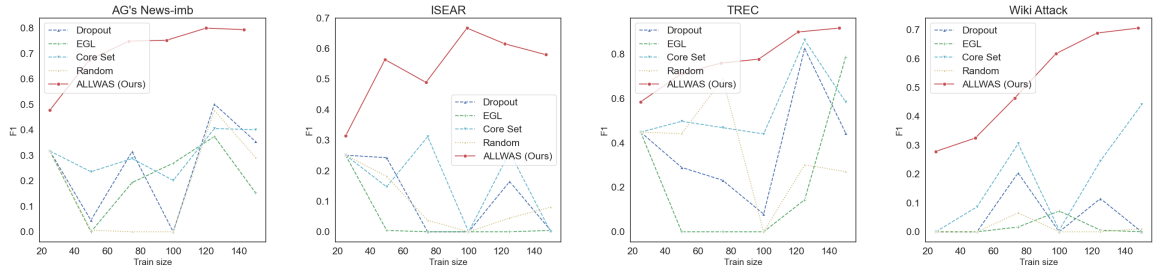


Figure 3: Results on the Imbalanced Practical setting. Our Model clearly outperforms the baselines.

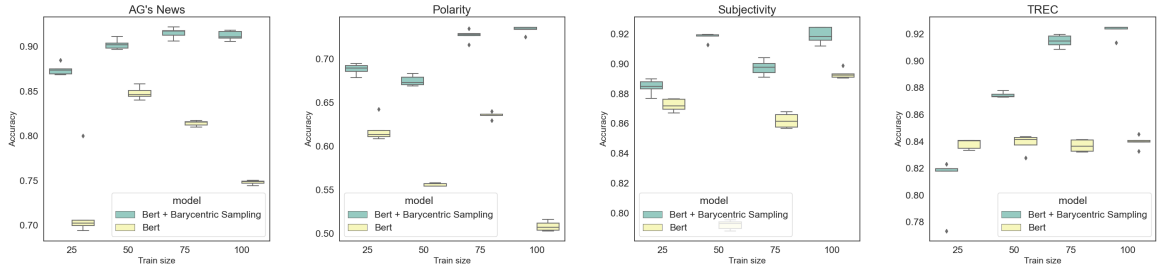


Figure 4: Few sample setting. Our setting (BERT+barycentric sampling) illustrates superior performance.

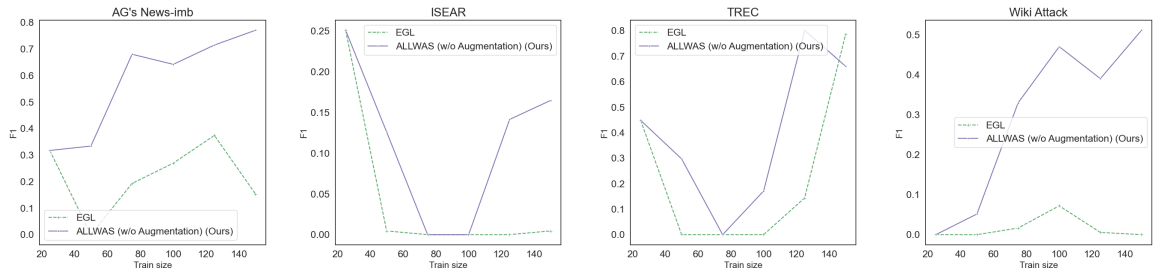


Figure 5: Comparison between selection based on maximum and coresets in the gradient domain

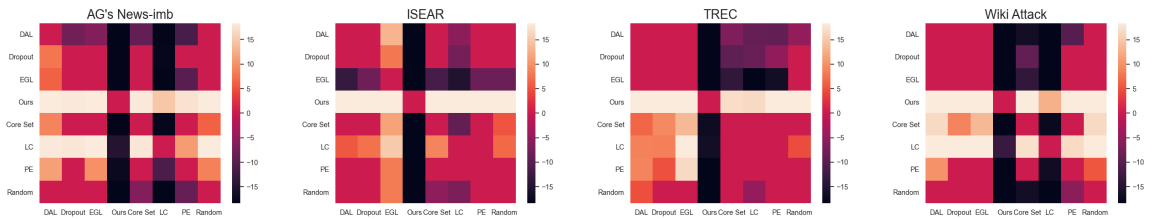


Figure 6: Statistical significance. Our model is statistically significant compared to baseline, illustrating the robustness of our proposed approach.

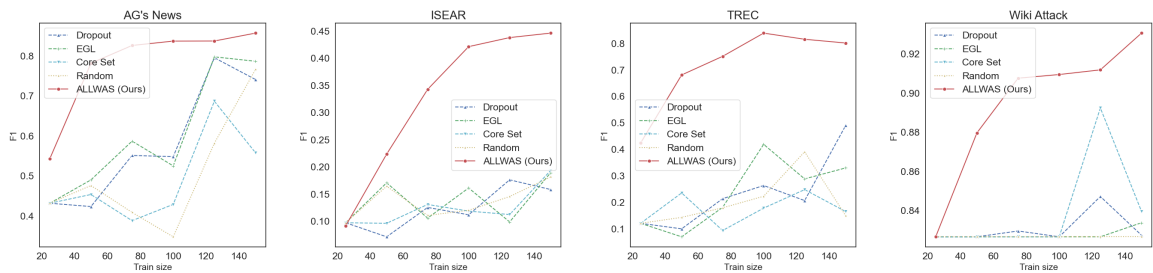


Figure 7: Results on the Multiclass setting. Our model performs significantly better than baselines.

Sampling from ℓ_2 is done by performing a kernel density estimation in the embedding space and then sampling from the resulting distribution. We report the Wilcoxon signed-rank test statistics in table 1 with Bonferroni correction to take into account the runs from all the datasets, settings, and iterations. Statistically significant (better) results are reported of the two sampling techniques against each other and a control of no over-sampling (augmentation). The results indicate that while both the over-sampling methods perform better than no sampling, reaffirming **RQ2**, sampling from the Wasserstein barycenter performs better than sampling from the ℓ_2 barycenter confirming the claim in 3.2.1 and asserting **RQ4**.

Significance wrt	ℓ_2	Wasserstein
No over-sampling	$< 10^{-20}$	$< 10^{-26}$
ℓ_2	-	$< 10^{-12}$
Wasserstein	-	-

Table 1: Comparison of over-sampling (for augmentation) from the ℓ_2 vs Wasserstein barycenters, indicating p-values if the method of the column is significantly better than that of the row. - indicates statistically insignificant or worse performance

5.5 Statistical Significance

We study if the performance of our methods is statistically significant concerning the baselines for each dataset. We perform the Wilcoxon signed-rank test for significance with Bonferroni correction. We select the Wilcoxon test due to its non-parametric nature. The significant results in the form of heatmaps of the logarithms of the p-values are shown in figure 6. The insignificant results have their values at 0. From the heatmaps, our method outperforms the baselines in all datasets, indicating the increase is indeed statistically significant. The results echo the observation made by (Ein-Dor et al., 2020) that no single sampling strategy is better than all others. However, in the low data regime that we operate in, many of the methods are not significantly better than the random sampling baseline.

5.6 Multi class Active Learning Results

Similar to the binary settings, we also study the performance of our method in the multi-class setting. We find that in the multi-class setting, too,

our method works better than the baselines, as can be seen in figure 11. This shows that our method is not restricted to the binary classification setting but also to the more generic multi-class cases.

5.7 Effect of augmentation factor

We study the effect of the multiplicative factor while augmenting the samples using barycentric sampling technique. Here the number of samples of which to compute the barycenter is kept at two. The results are given in the appendix. It is observed that as the augmentation factor is increased, the performance increases initially when the data is low. However, as more data is acquired from the unlabeled pool, the gap reduces. This indicates that we may benefit more by keeping the augmentation factor high in the low data regime.

5.8 Effect of number of samples to find the barycenter

Similar to subsection 5.7, we study the effect of the number of data points used to find the barycenter. Keeping the augmentation factor fixed at 20, we vary the number of samples to find the barycenter. Results are in the Appendix. It is observed that as the data points to the sample increases, the performance marginally drops. This becomes intuitive if we think of computing the barycenter as averaging over the samples. If we average out many samples, we effectively get the representative sample which would be similar in most iterations.

6 Conclusion

This paper presents and studies novel approaches of data sampling using concepts from submodular optimization and optimal transport theory for active learning in language models. We find that augmenting data using the Wasserstein barycenter helps to learn in the few sample setting. Further, we conclude that using a submodular function based on the Wasserstein distance for sampling in the gradient domain helps in active learning. Future works could explore data subset distances using optimal transport to find the subset of data that would benefit the model. It also remains to be explored if using core-sets obtained in this manner would help speed up the training of language models without affecting its accuracy by a large margin. We point readers to the open questions in this domain as next viable steps.

593

594

595

596

597

598

599

600

601

602

603

604

605

606

607

608

609

610

611

612

613

614

615

616

617

618

619

620

621

622

623

624

625

626

627

628

629

630

631

632

633

634

635

636

637

638

639

640

641

642

643

644

645

646

References

Martial Agueh and Guillaume Carlier. 2011. [Barycenters in the wasserstein space](#). *SIAM Journal on Mathematical Analysis*, 43(2):904–924.

Iaroslav Beshpalov, Nazar Buzun, Oleg Kachan, and Dmitry V. Dylov. 2021. [Data augmentation with manifold barycenters](#).

Yuxin Chen and Andreas Krause. 2013. [Near-optimal batch mode active learning and adaptive submodular optimization](#). In *Proceedings of the 30th International Conference on Machine Learning*, volume 28 of *Proceedings of Machine Learning Research*, pages 160–168, Atlanta, Georgia, USA. PMLR.

Michael B. Cohen, Cameron Musco, and Christopher Musco. 2017. [Input sparsity time low-rank approximation via ridge leverage score sampling](#). In *Proceedings of the Twenty-Eighth Annual ACM-SIAM Symposium on Discrete Algorithms*, SODA ’17, page 1758–1777, USA. Society for Industrial and Applied Mathematics.

David A. Cohn, Zoubin Ghahramani, and Michael I. Jordan. 1996. [Active learning with statistical models](#). *J. Artif. Int. Res.*, 4(1):129–145.

Marco Cuturi and Arnaud Doucet. 2014. [Fast computation of wasserstein barycenters](#). In *Proceedings of the 31st International Conference on Machine Learning*, volume 32 of *Proceedings of Machine Learning Research*, pages 685–693, Beijing, China. PMLR.

Jacob Devlin, Ming-Wei Chang, Kenton Lee, and Kristina Toutanova. 2019. [BERT: Pre-training of deep bidirectional transformers for language understanding](#). In *Proceedings of the 2019 Conference of the North American Chapter of the Association for Computational Linguistics: Human Language Technologies, Volume 1 (Long and Short Papers)*, pages 4171–4186, Minneapolis, Minnesota. Association for Computational Linguistics.

Mladen Dimovski, Claudiu Musat, Vladimir Ilievski, Andreea Hossmann, and Michael Baeriswyl. 2018. [Submodularity-inspired data selection for goal-oriented chatbot training based on sentence embeddings](#). In *Proceedings of the 27th International Joint Conference on Artificial Intelligence*, IJCAI’18, page 4019–4025. AAAI Press.

Liat Ein-Dor, Alon Halfon, Ariel Gera, Eyal Shnarch, Lena Dankin, Leshem Choshen, Marina Danilevsky, Ranit Aharonov, Yoav Katz, and Noam Slonim. 2020. [Active learning for BERT: An empirical study](#). In *Proceedings of the 2020 Conference on Empirical Methods in Natural Language Processing (EMNLP)*, pages 7949–7962, Online. Association for Computational Linguistics.

Steven Y Feng, Varun Gangal, Jason Wei, Sarath Chandar, Soroush Vosoughi, Teruko Mitamura, and Edward Hovy. 2021. [A survey of data augmentation approaches for nlp](#). *arXiv e-prints*, pages arXiv–2105. 647
648
649
650

Yarin Gal and Zoubin Ghahramani. 2016. [Dropout as a bayesian approximation: Representing model uncertainty in deep learning](#). In *Proceedings of The 33rd International Conference on Machine Learning*, volume 48 of *Proceedings of Machine Learning Research*, pages 1050–1059, New York, New York, USA. PMLR. 651
652
653
654
655
656
657

Daniel Gissin and Shai Shalev-Shwartz. 2019. [Discriminative active learning](#). *CoRR*, abs/1907.06347. 658
659

Chuan Guo, Geoff Pleiss, Yu Sun, and Kilian Q. Weinberger. 2017. [On calibration of modern neural networks](#). *CoRR*, abs/1706.04599. 660
661
662

Gholamreza Haffari and Anoop Sarkar. 2009. [Active learning for multilingual statistical machine translation](#). In *Proceedings of the Joint Conference of the 47th Annual Meeting of the ACL and the 4th International Joint Conference on Natural Language Processing of the AFNLP*, pages 181–189, Suntec, Singapore. Association for Computational Linguistics. 663
664
665
666
667
668
669
670

Sariel Har-Peled and Soham Mazumdar. 2004. [On coresets for k-means and k-median clustering](#). In *Proceedings of the Thirty-Sixth Annual ACM Symposium on Theory of Computing*, STOC ’04, page 291–300, New York, NY, USA. Association for Computing Machinery. 671
672
673
674
675
676

Steven C. H. Hoi, Rong Jin, and Michael R. Lyu. 2006. [Large-scale text categorization by batch mode active learning](#). In *Proceedings of the 15th International Conference on World Wide Web*, WWW ’06, page 633–642, New York, NY, USA. Association for Computing Machinery. 677
678
679
680
681
682

Wei-Ning Hsu and Hsuan-Tien Lin. 2015. [Active learning by learning](#). 683
684

Jiayi Huang, Rewon Child, Vinay Rao, Hairong Liu, Sanjeev Satheesh, and Adam Coates. 2016. [Active learning for speech recognition: the power of gradients](#). *CoRR*, abs/1612.03226. 685
686
687
688

Angelos Katharopoulos and François Fleuret. 2019. [Not all samples are created equal: Deep learning with importance sampling](#). 689
690
691

Leonard Kaufman and Peter J. Rousseeuw. 1987. [Clustering by means of medoids](#). 692
693

Katrin Kirchhoff and Jeff Bilmes. [Submodularity for data selection in statistical machine translation](#). 694
695

Sosuke Kobayashi. 2018. [Contextual augmentation: Data augmentation by words with paradigmatic relations](#). In *Proceedings of the 2018 Conference of the North American Chapter of the Association for* 696
697
698
699

807	Dan Shen, Jie Zhang, Jian Su, Guodong Zhou, and Chew-Lim Tan. 2004. Multi-criteria-based active learning for named entity recognition . In <i>Proceedings of the 42nd Annual Meeting of the Association for Computational Linguistics (ACL-04)</i> , pages 589–596, Barcelona, Spain.	862
808		863
809		864
810		865
811		866
812		867
813	Aditya Siddhant and Zachary C. Lipton. 2018. Deep bayesian active learning for natural language processing: Results of a large-scale empirical study . <i>CoRR</i> , abs/1808.05697.	868
814		869
815		870
816		871
817	Katrin Tomanek and Udo Hahn. 2009. Reducing class imbalance during active learning for named entity annotation . In <i>Proceedings of the Fifth International Conference on Knowledge Capture, K-CAP '09</i> , page 105–112, New York, NY, USA. Association for Computing Machinery.	872
818		873
819		874
820		875
821		876
822		877
823	Simon Tong and Daphne Koller. 2002. Support vector machine active learning with applications to text classification . <i>J. Mach. Learn. Res.</i> , 2:45–66.	878
824		879
825		880
826	C. Villani. <i>Optimal transport: old and new</i> , volume 338. Springer Verlag.	881
827		882
828	William Yang Wang and Diyi Yang. 2015. That’s so annoying!!!: A lexical and frame-semantic embedding based data augmentation approach to automatic categorization of annoying behaviors using #petpeeve tweets . In <i>Proceedings of the 2015 Conference on Empirical Methods in Natural Language Processing</i> , pages 2557–2563, Lisbon, Portugal. Association for Computational Linguistics.	883
829		884
830		885
831		886
832		887
833		888
834		889
835		890
836	Alex Warstadt, Amanpreet Singh, and Samuel R. Bowman. 2019. Neural network acceptability judgments . <i>Transactions of the Association for Computational Linguistics</i> , 7:625–641.	891
837		892
838		893
839		894
840	Kai Wei, Rishabh Iyer, and Jeff Bilmes. 2015. Submodularity in data subset selection and active learning . In <i>Proceedings of the 32nd International Conference on Machine Learning</i> , volume 37 of <i>Proceedings of Machine Learning Research</i> , pages 1954–1963, Lille, France. PMLR.	895
841		896
842		897
843		898
844		899
845		900
846	Ellery Wulczyn, Nithum Thain, and Lucas Dixon. 2017. Ex machina: Personal attacks seen at scale . In <i>Proceedings of the 26th International Conference on World Wide Web, WWW '17</i> , page 1391–1399, Republic and Canton of Geneva, CHE. International World Wide Web Conferences Steering Committee.	901
847		902
848		903
849		904
850		905
851		906
852	Zuobing Xu, Ram Akella, and Yi Zhang. 2007. Incorporating diversity and density in active learning for relevance feedback. In <i>Advances in Information Retrieval</i> , pages 246–257, Berlin, Heidelberg. Springer Berlin Heidelberg.	907
853		908
854		909
855		910
856		911
857	Yuguang Yan, Mingkui Tan, Yanwu Xu, Jiezhong Cao, Michael Ng, Huaqing Min, and Qingyao Wu. 2019. Oversampling for imbalanced data via optimal transport . <i>Proceedings of the AAAI Conference on Artificial Intelligence</i> , 33(01):5605–5612.	912
858		913
859		
860		
861		
	Xiang Zhang, Junbo Zhao, and Yann LeCun. 2015. Character-level convolutional networks for text classification. In <i>Proceedings of the 28th International Conference on Neural Information Processing Systems - Volume 1, NIPS'15</i> , page 649–657, Cambridge, MA, USA. MIT Press.	
	Jianchao Zhu, Liangliang Shi, Junchi Yan, and Hongyuan Zha. 2020. Automix: Mixup networks for sample interpolation via cooperative barycenter learning. In <i>Computer Vision – ECCV 2020</i> , pages 633–649, Cham. Springer International Publishing.	
	A Appendix	
	A.1 Details of Dataset	
	We use seven standard text classification datasets and their ten variants as used by (Ein-Dor et al., 2020). Specifically, the datasets used are Wiki Attack (Wulczyn et al., 2017) which annotates wikipedia discussions for offensive content, ISEAR (Shao et al., 2015) which reports for personal accounts of emotions, TREC (Shao et al., 2015) which classifies question categories, CoLA (Warstadt et al., 2019) which identifies the content for linguistic acceptability, AG’s News (Zhang et al., 2015) which categorises news articles, Subjectivity (Pang and Lee, 2004) which classifies movie snippets into subjective and objective and Polarity (Pang and Lee, 2005) which provides sentiment categories of movie reviews. The datasets which contain labels with a prior of greater than 15% are taken into the balanced setting and those with less than a 15% prior are considered in the imbalanced setting as in (Ein-Dor et al., 2020). The experimental setup considers 3 settings: (1) Balanced , in which the prior probability of a class occurrence is $\geq 15\%$. Here the initial seed for labeling is obtained by random sampling. (2) Imbalanced and (3) Imbalanced practical in which the prior probability of a class occurrence is $\leq 15\%$. In the case of the Imbalanced setting the initial seed is taken by randomly sampling from the class with the low prior. Here the assumption is that there exists a heuristic to obtain an unbiased sample set with high precision of the low prior class. As this may not always hold true the Imbalanced practical setting samples using a simple and empirical heuristic such as a query based search for the samples belonging to the low prior class. This gives a (biased) set of samples of the class which are then used for labeling. For the class with a high prior probability random samples are drawn from the dataset and are labeled as such for both the imbalanced settings.	

No.	Dataset	Size	Class	Prior
1	Subjectivity-imb	5,556	subjective	10%
2	Polarity-imb	5,923	positive	10%
3	AG's News-imb	17,538	world	10%
4	Wiki attack	21,000	general	12%
5	ISEAR	7,666	fear	14%
6	TREC	5,952	location	15%
7	AG's News	21,000	world	25%
8	CoLA	9,594	unacceptable	30%
9	Subjectivity	10,000	subjective	50%
10	Polarity	10,662	positive	50%

Table 2: Dataset Statistics

A.2 Details of Comparative Methods

The acquisition methods are used to query and obtain samples from the unlabeled pool for labeling. In the implementation 25 samples are queried per iteration. We use the active learning acquisition strategies as in (Ein-Dor et al., 2020) as below:

1. **Random**: The data for labeling are randomly sampled from the unlabeled pool.
2. **Least Confidence (LC, (Lewis and Gale, 1994))**: This method picks the top k samples for which the model uncertainty is the highest.
3. **Monte Carlo Dropout (Dropout, (Gal and Ghahramani, 2016))**: This uses Monte Carlo dropout during inference for multiple runs and averages the probabilities followed by sampling the least certain instances.
4. **Perceptron Ensemble (PE, (Ein-Dor et al., 2020))**: Here the output of an ensemble of models is used to pick the instances with highest uncertainty. To avoid the computational cost associated with training an ensemble of BERT models, this method uses the perceptron models trained on the CLS output of the finetuned BERT.
5. **Expected Gradient Length (EGL, (Huang et al., 2016))**: The samples are selected based on the largest expected gradient norm as in (Huang et al., 2016). The expectation is over the model predicted probabilities.
6. **Core-Set ((Sener and Savarese, 2018))**: This method picks samples that best cover the dataset in the embedding space (CLS) using the greedy method described in (Sener and Savarese, 2018).
7. **Discriminative Active Learning (DAL, (Gissin and Shalev-Shwartz, 2019))**: This technique selects samples that make the L most representative instances of the entire pool as per (Gissin and Shalev-Shwartz,

2019).

A.3 Additional Results

A.3.1 Active Learning Results on the Binary class settings

The results for the three binary settings are shown in the graphs in figures 8, 9 and 10. From the figures we observe that in most of the datasets our method outperforms all the other methods in all settings. We report the f_1 scores for all settings, since in the balanced case also there may be a slight class imbalance (upto 60%). For the balanced setting we find that our method performs exceptionally well in the start with lesser data and then as the training data increases with iterations the performance of the other methods catch up. Thus we could say that our method converges faster in scenarios where the data is balanced. There was one exception with the Cola dataset in which the metric drops as compared to others. Upon further investigating we find that the upsampling causes a drop in performance in this case. Thus, while sampling in this manner may cause an increase in performance in most of the cases it may require the practitioner to fine tune the factor by which to augment the data. In the other 2 settings, namely the imbalanced settings, we observe a clear gain in performance. Thus we conclude that the combination of our submodular query function and barycentric sampling benefits performance in active learning scenarios where there is prevalence of class imbalance.

A.3.2 Multi class Active Learning Results

In addition to the results in the main paper, here we report the results on all methods for the multi-class setting in figure 11.

A.3.3 Effect of augmentation factor

We would like to study the effect of the multiplicative factor while augmenting the samples using barycentric sampling technique. Here the number of samples of which to compute the barycenter are kept at 2. The results are shown in figure 12. It can be seen that as the augmentation factor is increased the performance increases initially, when the data is low, but as more data is acquired from the unlabeled pool the gap reduces and also reverses. This indicates that we may benefit more by keeping the augmentation factor high in the low data regime.

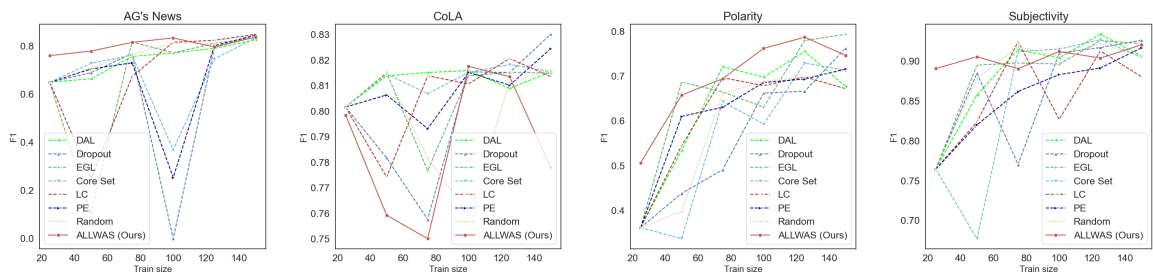


Figure 8: Results on the Balanced setting

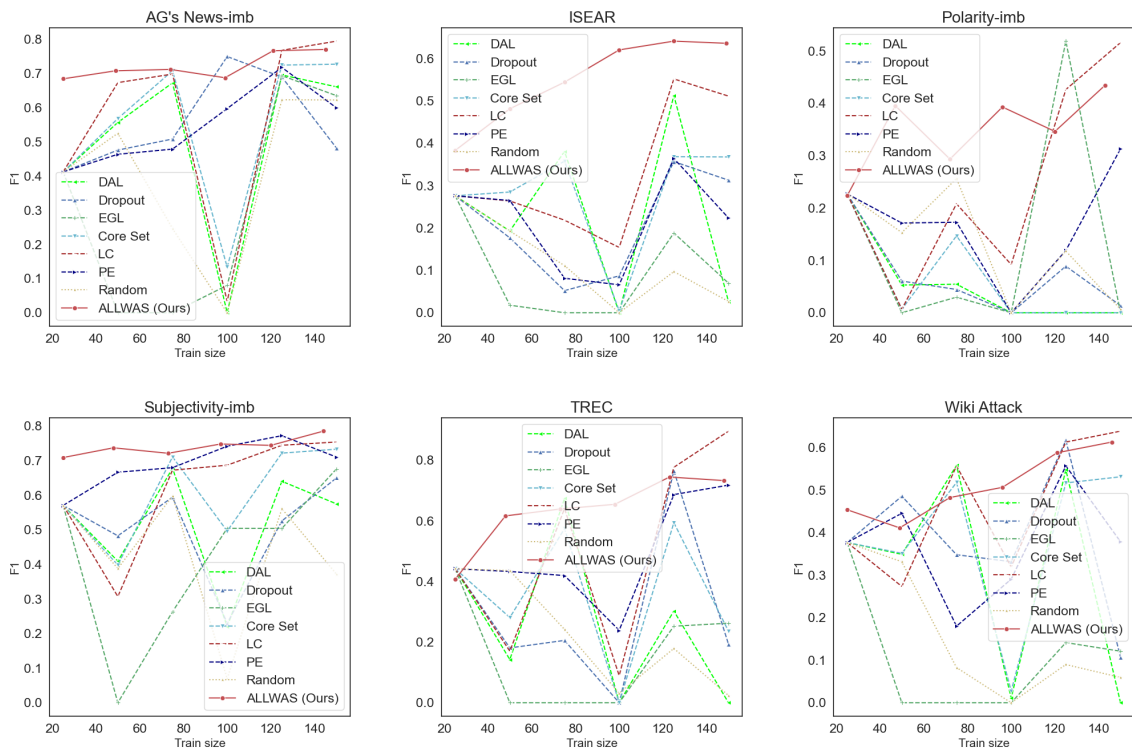


Figure 9: Results on the Imbalanced setting

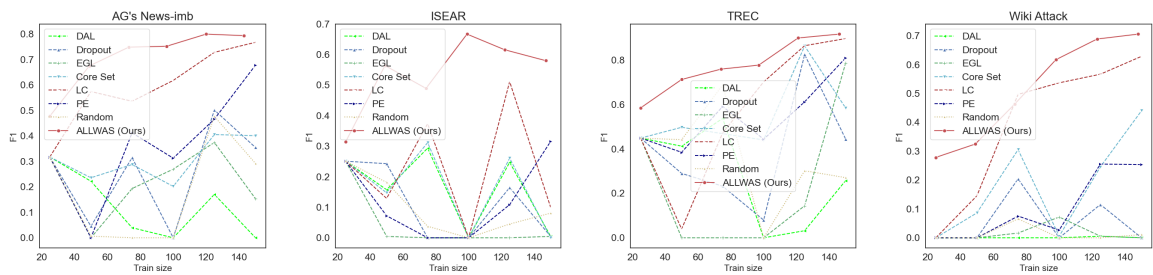


Figure 10: Results on the Imbalanced Practical setting

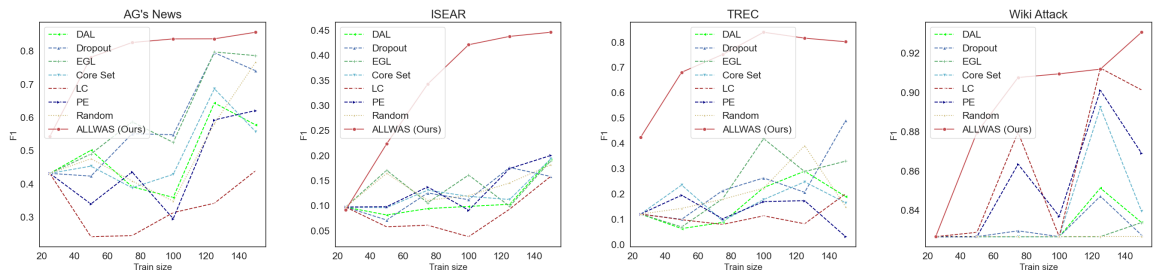


Figure 11: Results in the Multi-class setting

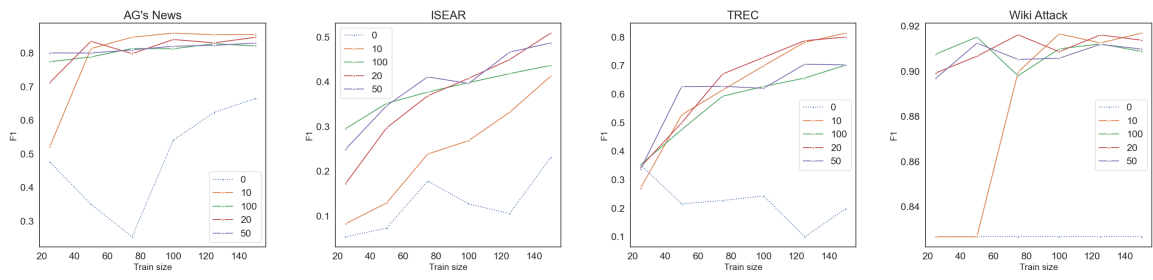


Figure 12: Ablation study on the augmentation factor

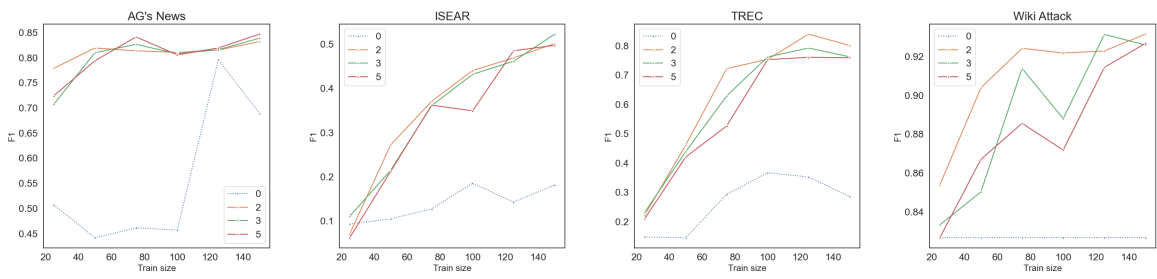


Figure 13: Ablation study on the number of samples to compute the barycenter

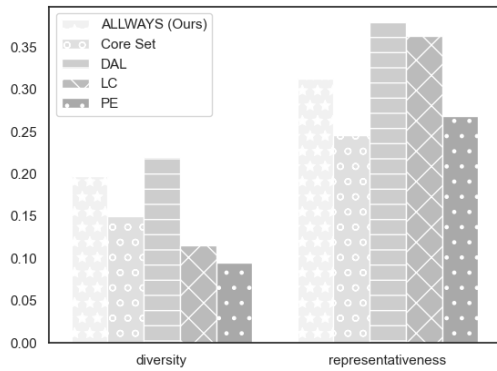


Figure 14: Diversity and Representativeness

1001 **A.3.4 Effect of number of samples to find the** 1002 **barycenter**

1003 Similar to section A.3.3, we would like to study
1004 the effect of the number of data points used to find
1005 the barycenter. Keeping the augmentation factor
1006 fixed at 20, we vary the number of samples to find
1007 the barycenter. As can be seen in figure 13, it can
1008 be understood that as the data points to sample
1009 from increases the performance marginally drops.
1010 This becomes intuitive if we think of computing
1011 the barycenter as averaging over the samples and
1012 if we average out many samples we effectively get
1013 the representative sample which would similar in
1014 most iterations especially in the labels space.

1015 **A.3.5 Diversity and Representativeness**

1016 We compute the diversity and representativeness
1017 of the selected samples as outlined in (Ein-Dor
1018 et al., 2020). From figure 14 we see that our
1019 method gives comparable values of these metrics.
1020 DAL performs well on both the metrics as it was
1021 designed for maximising them. This shows there
1022 is some room for improvement in the proposed
1023 method with regards to the diversity and represen-
1024 tiveness metrics. We leave this for future works.